



EGYPTIAN ACADEMIC JOURNAL OF
BIOLOGICAL SCIENCES
ZOOLOGY

B

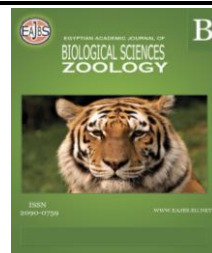


ISSN
2090-0759

WWW.EAJBS.EG.NET

Vol. 14 No. 1 (2022)

www.eajbs.eg.net



Biochemical, Molecular and Histopathological Studies on Malathion Toxicity on Some Vital Organs of Male Rats

Nourhan Morsi¹, Mohamed Wassem¹, Mahmoud Badr² and AbdelKarim Abdel Latif¹

1-Faculty of Science, Fayoum University, Zoology department (Cytology, Histology and Genetics), Fayoum, Egypt.

2-Poisoning Control Center, Ain Shams University Hospitals, Cairo, Egypt

E-mail*: na1737@fayoum.edu.eg

ARTICLE INFO

Article History

Received:21/2/2022

Accepted:12/4/2022

Available:14/4/2022

Keywords:

Malathion,
antioxidants, mRNA
expression of
P⁵³ and P²¹,
Immunohistochemistry

ABSTRACT

Malathion is an organophosphorus pesticide widely used throughout agriculture and veterinary practices. The present study aimed to evaluate the toxic effects of Malathion inhalation through simulation of three models of environmental toxicity in different exposure periods of acute, chronic, and subchronic doses. The histological, immunohistochemical examinations of the morphological integrity of the liver and brain, together with some biochemical (TAC, CAT, SOD, GPx and Se) and molecular (Real-time PCR for p53 and P21 mRNA) studies will be assessed to highlight the effects of the studied sub-lethal doses of Malathion. Four groups of male Wister rats were used in the experiment one for the control group and the others for subchronic, chronic and acute doses. Many toxic symptoms, a significant decrease in CAT, CAT, SOD, GPx and Se values. Malathion cause also significant disturbance in different comet assay parameters in both blood and liver tissue cells. Also, Real-time PCR for mRNA of P53 and P21 in the liver showed a significant increase in mRNA expression of P53 and P21 and a significant decrease in mRNA expression of P53 and P21 in brain tissue. P53 immunohistochemistry in liver tissue shows an increase in its activity and a decrease in hippocampus tissue cells. Many histopathological lesions such as inflammation, vacuolation, apoptosis, necrosis, and fibrosis of the hepatic tissue cells, were recorded in all treated groups.

INTRODUCTION

Malathion (M) is an organophosphorus (OP) insecticide and pesticide commonly used in crops and residential applications. The negative effects of Malathion on human health and ecosystems are of great concern. Malathion is one of the most widely used OP pesticides due to its high selectivity to pests and low toxicity to human (Poomagal *et al.*, 2021). Organophosphate insecticides (OPI) are more toxic to vertebrates with low mammalian toxicity (Shah *et al.*, 2010, Balali *et al.*, 2012). The primary mechanism of (OPI) induced toxicity is

related to acetylcholinesterase (AChE) inhibition (Tchounwou *et al.*, 2015). Further, the toxicity of OP agents may be due to the formation of reactive oxygen species (ROS), leading to lipid peroxidation (LPO) as it was provoked by deltamethrin in the previous works (Issam *et al.*, 2009), which is generally assessed by an increase in the levels of thiobarbituric acid reactive substances (TBARS) (Hazarika *et al.*, 2003; Banerjee *et al.*, 1999; Verma & Srivastava 2001). Malathion is an organophosphorus compound that is lipophilic and it is evident that LPO is accompanied by an alteration (inhibition or activation) in the antioxidant defense system in different organs, including the liver (Hazarika *et al.* 2003; Srikanth & Seth 1990; Fortunato *et al.* 2006). Malathion (O, O-dimethyl phosphorodithioate of diethyl mercaptosuccinate) is the most famous example of (OPI), which is a non-systemic broad-spectrum insecticide used widely in agriculture (Ojha & Srivastava, 2014).

The International Agency for Research on Cancer (IARC) classified malathion and diazinon as probably carcinogenic to humans (group 2A) and dichlorvos, parathion, and tetrachlorvinphos as possibly carcinogenic to humans (group 2B) (Guyton *et al.*, 2015). In addition, several studies have highlighted oxidative stress as a possible underlying mechanism of malathion toxicity through increasing the production of reactive oxygen species (ROS) and subsequent membrane lipid peroxidation (Coban *et al.*, 2015). The total antioxidant capacity (TAC) measures the capacity of a biological sample (plasma, tissue extract) to inhibit the transformation of a selected substrate by an in vitro generated free radical since the antioxidant systems can act in a cooperative way (Winston *et al.*, 1998). The role and effectiveness of the first line defense antioxidants which basically include superoxide dismutase (SOD), catalase (CAT) and glutathione peroxidase (GPX) is important and indispensable in the entire defense strategy of antioxidants, especially in reference to superoxide anion radical (O_2^-) which is perpetually generated in normal body metabolism, particularly through the mitochondrial energy production pathway (MEPP) (Ighodaro & Akinloye, 2018). Selenium (Se) an essential trace element for animals and humans, it is involved in the complex system of defense against oxidative stress through selenium-dependent glutathione peroxidases (GPx) and other selenoproteins (Pennanen *et al.*, 2002). When DNA is damaged, cell division will stagnate in the G1 phase of the cell cycle, so the checkpoint is extremely important in this phase. P^{53} is a tumor suppressor gene that is involved in the G1-S checkpoint and has the function of gene guards. The p21 gene is lying in the downstream position of the p53 gene in the signaling pathway and is a cyclin-dependent kinase inhibitor (CDKI), p21 and p53 constitute the G1-S checkpoints, so damaged cells stagnate in the G1 phase to reduce the formation of mutations and thus play a tumor suppressor effect (Qiu *et al.*, 2008).

Therefore, with the consideration as a prototype of OP's, Malathion was selected as a toxic substance to create toxicity in our present study.

MATERIALS AND METHODS

Chemicals:

Malathion used here is (dimethoxythiophosphorylthio) succinate commercially available as malathion coromandel 57% was obtained from Kafr ElZayat company, Egypt. Quantitative determination of plasma TAC level and plasma aGPX activity was carried out by a colorimetric method using a kit provided by Biodiagnostic, (Egypt).

Quantitative determination of Selenium (Se) was determined in the faculty of agriculture, Fayoum University according to Environmental protection agency (Environmental protection agency, 1996).

Animals:

The study was performed on fifty-six adult male Wistar rats, weighing $100\text{g} \pm 20\text{g}$, supplied by the Animal House of Helwan University, Helwan, Egypt. The animals were housed in polypropylene cages under fully hygienic conditions and had free access to fresh water and fresh well-balanced food. This study was conducted according to the guiding principles of Animal Care.

Experimental Design:

After one week of acclimatization to the laboratory conditions.

Fifty-six male rats were randomly divided into four groups of 14 rats (5 rats per cage) as follows:

Group 1: is a control group.

Group 2: Rats were inhaled 0.1375 mg/kg body weight as $1/10$ of LD₅₀ for 30 days as a subchronic group.

Group 3: Rats were inhaled at 0.2062 mg/kg body weight) as $1/15$ of LD₅₀ for 90 days as a chronic group.

Group 4: Rats were inhaled 5.3 mg/kg body weight for 10 days as an acute group.

Rats were inhaling Malathion which was sprayed from air holes in cages which covered for 5 min.

Sample Collection and Preparation:

Rats were anesthetized by inhalation of diethyl ether then rats of all experimental groups were anesthetized and sacrificed. Blood and tissue samples were collected from them. Heparin was used as an anticoagulant for white blood cells (WBCs) and plasma samples which were obtained by centrifugation at 3000 rpm for 15 min and Samples were stored at -30°C until use for subsequent biochemical analysis of DNA damage assay and (Plasma catalase (CAT), erythrocyte lysate superoxide dismutase (SOD), erythrocyte lysate glutathione peroxidase (GPx) level, Total antioxidant capacity (CAT) & Selenium (Se) as oxidative markers (enzymatic and non-enzymatic antioxidants)) (Awadalla & Salah-Eldin, 2016).

Tissues Analysis:

- 1- The liver and brain were immediately removed; 0.5 grams of the liver are immediately frozen at -30°C with the hippocampus part of the brain in two different eppendorf.
- 2- Moreover, sections of the liver and brain are washed using chilled saline solution. Then tissues were preserved in formalin (10%, w/v) for the histological parameter.
- 3- The livers and the blood of both test and control were dissected and placed in eppendorf tubes containing ice-cold PBS. The liver tissues were then washed and minced with scissors to release single cells from liver tissues in PBS buffer with 20 mM EDTA. The layer with cell suspension was separated in a new tube after settling tissues pieces and cell debris from the sample. The cells were counted, washed in ice-cold PBS and adjusted to 1×10^5 cells/ ml.

Antioxidant Enzyme Assays:

Measurement of TAC:

The determination of the antioxidative capacity is performed by the reaction of antioxidants in the sample with a defined amount of exogenously provided H₂O₂ according to the method of Koracevic (Koracevic *et al.*, 2001).

Measurement of CAT Activity:

CAT activity was measured according to the method of Aebi (1984) as the rate constant of hydrogen peroxide (H₂O₂) decomposition. The activity was monitored at 510 nm.

Measurement of SOD Activity:

Superoxide dismutase activity is determined by Nishikimi (Nishikimi *et al.*, 1972).

Measurement of GPx Activity:

GPx activity was measured according to the method of Paglia and Valentine (1967).

Measurement of Se

Selenium element was determined according to the Environmental protection agency (1996).

Comet Assay:

This was performed after (Singh *et al.*, 1988) and (Olive *et al.*, 1990) with modifications. All steps were done in a faint light to reduce the UV damage. The low melting point agarose (0.8 % in PBS) was warmed in boiled water and allowing it to return to 37 °C then mixed with the isolated liver cells in a 1:10 ratio. The mixture was then added to a fully frosted microscope slides coated with 110 µl of normal melting point agarose (1% in PBS). The software provided several parameters but tail DNA content (Measured in PX from the center of the nucleus to the end of the tail) and Olive tail moment (OTM) was considered to be the important parameters (Kumaravel & Jha, 2006).

Detection of Gene Expression Level:

Perform all steps of RNA Purification of liver and brain cells according to (Nos, R. C. TRI Reagent®). The following sets of specific primers were employed for amplification of each cDNA: P53 (5`F-GTCGGCTCCGACTATAACACTATC-3`, 5`R-CTCTCTTTGCACTCCCTGGGGG-3`) (Saquib *et al.*, 2012), P21(5`F-GACCAGCATGACAGATTCTA CCA-3`, 5`R-TTCCTGTGGGCGGATTAGG-3`) (Ukpebor *et al.*, 2011) expression was normalized to GAPDH gene expression, which was used as an internal housekeeping control. Gene expression levels were calculated and determined following the formula of $2^{-\Delta\Delta Ct}$ ($\Delta Ct = Ct_{Gene} - Ct_{GAPDH}$; $\Delta\Delta Ct = \Delta Ct - \Delta Ct_{average\ normal\ controls}$).

Histopathological Examination:

Histological examination of testes was done. Specimens of the liver and the brain were fixed in neutral buffer formalin 10% and processed to get five-micrometer thick paraffin sections. The specimens were stained with hematoxylin and eosin after which they were passed through a mixture of equal concentrations of xylene and alcohol. Following clearance in xylene, the sections were oven-dried between 35°C and 40°C (Sheehan & Hrapchak, 1987), then examined by a light microscope.

P53 Immunohistochemistry:

Brain and liver tissue sections were deparaffinized in xylene and rehydrated in graded alcohol. Drops of Hydrogen Peroxide Block (Thermo Scientific, USA) were added to block the endogenous peroxidase activity. The quantitative immunoreactivity of P53 was evaluated in nuclear P53 stained cells. The expressions of P53 immunostaining were examined in different areas of the brain and liver tissue. The immunostained section was randomly counted in 10 microscopic fields under a high-power field (X400) microscope. In each field, positive cells and total cell numbers were recorded. The percentage of positively stained cells (%) was calculated. It was performed by Lica Q image analysis system.

RESULTS

Irritability, nervousness, diarrhea and frequent urination were observed in studied groups according to their doses subchronic, chronic and acute doses. Also, mortality had found during the experiment. Table (1) shows the Mortality rate of male Wister rats in the different studied groups through the experimental period. Table (2) shows the results of all antioxidant markers and they were highly statistically significant decreases in the subchronic, chronic and acute groups compared to the control group. Comet assay in the studied group's blood shows a comparison between the four groups as regards the values of %DNA in tail and tail moment in blood Table (3). Results of Table (4) show the comet assay analysis of the comparison between the four groups as regards the values of %DNA in tail and tail moment in the liver. That table shows the increase of tail moment as a result of the Malathion effect. mRNA expression levels of p21 and p53 genes in the liver Highly statistically significant increase in liver p21 and p53 gene levels in the subchronic, chronic and acute groups compared to the control group (Table 5). mRNA expression levels of p21 and p53 genes in the brain show a highly statistically significant decrease in brain p21 and p53 gene levels in the subchronic, chronic and acute groups compared to the control group (Table 6).

Table 1: Mortality rate of male Wister rats in the different studied groups through the experimental period.

		Duration of exposure	No. of dead rats	%
G1	Control (n=14)	-	0	0
G2	Sub Chronic dose(n=14)	30 days	0	0
G3	Chronic dose(n=14)	90 days	2	14
G4	Acute dose (n=14)	10 days	5	35

Table 2: Show the results of antioxidants markers levels in the different studied groups as regards the mean values of TAC, CAT, SOD,

Groups	TAC mmol/L	CAT U/L	SOD U/ml	GPx mu/ml	Se PPM
G1(control)	5.5 ± 0.30 ^A	714.3±24.64 ^A	107.2±13.92 ^A	63.3± 4.06 ^A	0.6± 0.021 ^A
G2(Subchronic)	4.6± 0.22 ^B	628.6±24.11 ^B	78.3±3.23 ^B	51.9± 2.51 ^B	0.4± 0.041 ^C
G3(Chronic)	2.8± 0.196 ^C	451.9±25.07 ^C	46.0±2.31 ^C	39.2± 1.71 ^C	0.4± 0.024 ^C
G4(Acute)	2.2± 0.186 ^C	190.3± 3.27 ^C	30.4±2.28 ^C	24.5± 1.21 ^C	0.3± 0.023 ^C

Each value is the mean of replicates ± standard error of means.

Groups with different letters have a statistically significant difference.

P^B= significant (P ≤ 0.05). P^C= highly significant (P ≤ 0.001). A= non-significant (P > 0.05).

Table 3: The results of comet assay analysis in blood including the mean value of % DNA in Head, Tail Length, % DNA in Tail and Tail Moment

Groups	% DNA in Head	Tail Length (px)	% DNA in Tail	Tail Moment
G 1(control)	90.5 ±0.7 ^A	3.3 ±0.4 ^A	9.5 ±0.8 ^A	0.8 ±0.03 ^A
G 2(subchronic)	81.27 ±0.5 ^B	5.7 ±0.9 ^B	18.8 ±0.2 ^B	1.4 ±0.07 ^B
G 3(chronic)	68.6 ±0.3 ^B	8.8 ±0.5 ^B	31.4 ±0.6 ^B	3.7 ±0.08 ^B
G 4(acute)	82.2 ±0.4 ^C	16.4 ±0.2 ^C	17.76 ±0.3 ^C	0.9 ±0.01 ^C

Groups with different letters have a statistically significant difference.

P^B= significant (P ≤ 0.05). P^C= highly significant (P ≤ 0.001). A= non-significant (P > 0.05)

Table 4: The results of comet assay analysis in the liver including the mean value of % DNA in Head, Tail Length, % DNA in Tail and Tail Moment

Groups	% DNA in Head	Tail Length (px)	% DNA in Tail	Tail Moment
G 1 (control)	80.8 ±0.6 ^A	4.5 ±0.2 ^A	19.2±0.8 ^A	0.98 ±0.07 ^A
G 2 (subchronic)	81.6 ±0.9 ^B	7.2 ±0.4 ^B	18.4 ±0.3 ^B	1.5 ±0.03 ^B
G3 (chronic)	78.7 ±0.2 ^B	4.2 ±0.5 ^B	21.3 ±0.4 ^B	1.02 ±0.02 ^B
G 4 (acute)	68.3 ±0.8 ^C	18.7 ±0.4 ^C	31.7 ±0.1 ^C	2.5 ±0.05 ^C

Groups with different letters have a statistically significant difference.

P^B= significant (P ≤ 0.05).

P^C= highly significant (P ≤ 0.001).

A= non-significant (P > 0.05)

Table 5: Results of mRNA expression levels of p21 and p53 genes in liver comparing the mean values of the four studied groups

Groups	Relative value of p21	Relative value of p53
G 1 (control)	1.0 ±0.05 ^A	0.99 ±0.1 ^A
G 2 (subchronic)	1.45 ±0.06 ^B	1.8 ±0.17 ^B
G 3 (chronic)	1.53 ±0.14 ^B	1.9 ±0.2 ^B
G 4 (acute)	1.61 ±0.12 ^C	2.2 ±0.2 ^C

Groups with different letters have a statistically significant difference.

P^B= significant (P ≤ 0.05).

P^C= highly significant (P ≤ 0.001).

A= non-significant (P > 0.05).

Table 6: Results of mRNA expression levels of p21 and p53 genes in the brain comparing the mean values of the four studied groups:

Groups	Relative value of p21	Relative value of p53
G 1 (control)	1.0 ±0.04 ^A	0.99 ±0.06 ^A
G 2 (subchronic)	0.8 ±0.06 ^B	0.66 ±0.07 ^B
G 3 (chronic)	0.78 ±0.03 ^B	0.64 ±0.08 ^B
G 4 (acute)	0.76 ±0.03 ^B	0.61 ±0.9 ^B

Groups with different letters have a statistically significant difference.

P^{*}= significant (P ≤ 0.05).

P^{**}= highly significant (P ≤ 0.001).

NS= non-significant (P > 0.05).

On microscopic examination, the H&E-stained liver tissues show the structural unit of the liver is the hepatic lobule which is made up of radiating strands of cells forming a network around a central vein (Fig. 1). Also shows main histopathological lesions dependent on their dose (Fig. 2) in subchronic dose liver showed mild pyknosis, karyorrhexis and karyolytic in hepatocytes also in cytoplasm showed the beginning of lymphocyte infiltration central vein dilatation was noticed in the subchronic group. In the chronic group, these histopathological changes increased plus hepatocytes hypertrophy and central vein dilatation and conjunction. In the acute group histopathological changes increased in addition to blood sinusoid dilatation, in the central vein and portal vein there is dilatation and conjunction, fibrosis in the portal area and hyperplasia in the bile duct. Immunohistochemical staining for p53 showed its normal distribution in the control group as a mild positive reaction in hepatocytes, marked mild reaction in the subchronic group, a moderate reaction in the chronic group and elevated in the acute group.

Histopathological Observations of the Liver Under Light Microscopy:

The liver cell strands are alternating with narrow blood sinusoids that also radially extend along the liver lobules, converging inwards to form the central or centrilobular veins. In the subchronic group, few leucocytic infiltrations and a few hepatocytes still appeared with cytoplasmic vacuolization and pyknotic, or karyolayzed nuclei were recorded. Kupffer and endothelial cells were hypertrophied with darkly stained nuclei. Paraffin section of the chronic group showed many histopathological alterations including loss of the liver architecture, the normal arrangement of the hepatocytes wasn't

easily recognized and some hepatic strands were dissociated. The studied liver sections of the acute group showed a higher tendency for loss of hepatic tissue structural pattern and fibrosis surrounding the dilated and congested portal vein and hyperplasia of the cells of bile ductules were also seen (Fig.1).

Immunohistochemical Results in the Studied Group's Liver:

The apoptotic cells were detected by the tumor suppressor gene P53 immunohistochemically as brown color. Immunohistochemical observation for P53 protein was undetectable in the nuclei of hepatocytes in the control group; the nuclei were stained with blue color (Fig. 2A). Nuclei of few numbers of hepatocytes give positive immune-reactivity as brown color in rats of the subchronic group, (Fig. 2B). Also, moderate p53 expressions have been seen in nuclei of hepatic cells of rats' liver (chronic group) (Fig. 2C). In contrast, an immunohistochemical study of the acute group revealed a strong positive reaction for the P53 gene in many numbers of hepatocytes (Fig. 2D)

Histopathological Results in The Studied Group's Brain:

H&E-stained sections of the control group revealed the C-shaped hippocampus was composed of the Cornu Ammonis (CA) in the form of CA1, CA2, CA3, CA4 and dentate gyrus (Fig. 3A). It was formed of pyramidal cells and astrocytes. CA1 region of the control group showed three layers; polymorphic, pyramidal, and molecular. The pyramidal cells appeared with large vesicular nuclei. Blood capillaries were noticed in the molecular and polymorphic layers (Fig. 3B). CA4 received afferent fibers while all fibers exit from CA1.

Light microscopic examination of the hippocampus in the CA3 region showed the thickness of the pyramidal layer and most of the neurocytes appeared normal (Fig. 3). Light microscopic examination of the hippocampus sections of the subchronic group showed a near-normal thickness of the pyramidal cell layer of the CA3 region with few pyramidal cells that appeared with pyknotic nuclei and vacuolar degenerated cytoplasm (Fig.3). Also, the hippocampus of the chronic group showed a moderate tissue change compared with other groups as mild diffuse vacuolar degeneration and pyknotic neurons or apoptotic pyramidal cells.

In contrast, paraffin sections from the rat hippocampus treated with 5.3 mg/kg bodyweight for 10 days of malathion showed numerous histopathological changes including the decreased thickness of the pyramidal cell layer in the CA3 region, a large number of damaged neurons, degenerated pyramidal cell, and vacuolated neurocytes. Nuclei of the cells were shrunken, pyknotic and hyperchromatic. Also; many damaged apoptotic astrocytes were in the form of pyknotic, shrunken and vacuolated neurons (Fig. 3.).

Immunohistochemical Results in The Studied Group's Brain:

Apoptotic cells were detected by the tumor suppressor gene P53 immunohistochemically as brown color. The CA3 region of the hippocampus stained with anti-p53 protein showed a negative or undetectable immunohistochemical reaction in the nuclei of hippocampus cells in the control group. The nuclei were stained with blue color (Fig.4A). Nuclei of few numbers of pyramidal or glial cells give positive immune-reactivity as brown color in rats of the subchronic group, (Fig. 4B). Also, moderate p53 expressions have been seen in nuclei of pyramidal or glial cells of rats of the chronic group (Fig. 4C). In contrast, the immunohistochemical study of the acute group revealed a strong positive reaction for the P53 gene in many numbers of pyramidal or glial cells of the hippocampus layer (Fig. 4D).

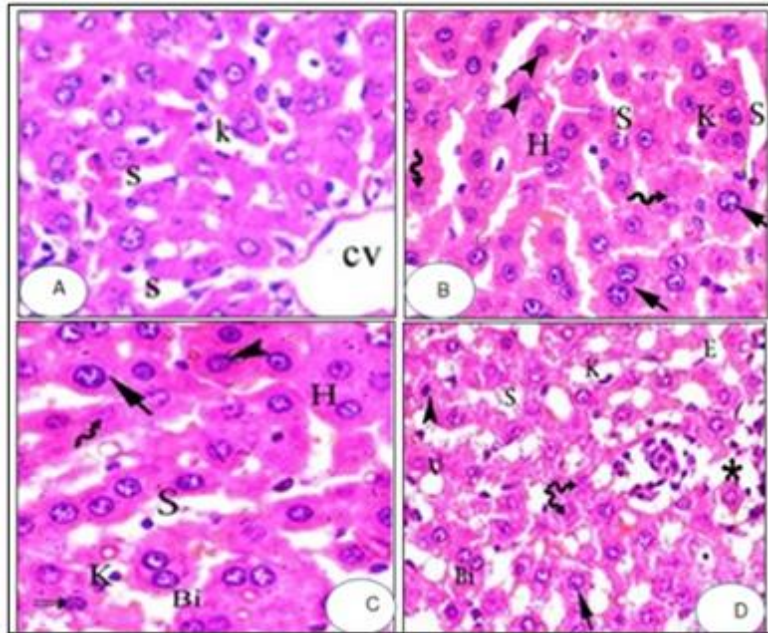


Fig 1: Photomicrographs of the section in the liver of chronic group 4 (rats treated with malathion) showing: A. mild dilated central vein (cv), surrounded by lymphocytes and small degenerated area (*) dilated blood sinusoids (S) and many hepatocytes with hypertrophied (arrow) or pyknotic nuclei (arrowhead) (HE, X 100). B. mild dilated portal vein (PV), with lymphocytic infiltration and bile ductules (BD) (HE, X 100). C. degenerated hepatocytes with mononuclear leucocytes infiltration (*), hepatocytes with highly vacuolated cytoplasm (V), dilated sinusoid (S) with hypertrophied and darkly stained kupffer cells (K). Many nuclear lesions were shown as binucleated (Bi), karyolysis (bent arrow) or karyorrhexis (double arrow), or pyknotic (arrowhead) (HE, X 400).

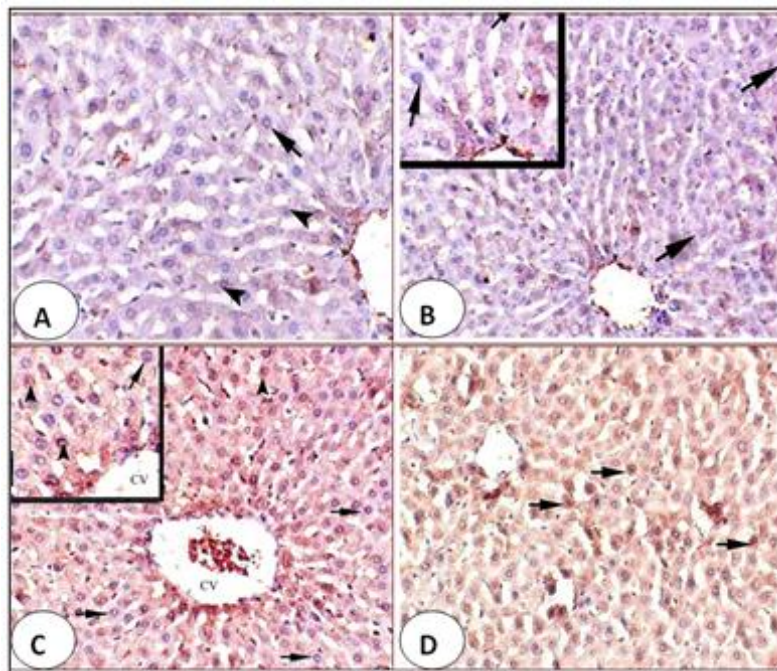


Fig.2. Photomicrographs of p53 immunoreactivity of different studied groups. A. The liver of the control group, B. The liver of the subchronic treated group. C. The liver of chronic and D in the acute group. The brown color represents a positive p53 reaction (arrowhead) while the blue color represents a nondetectable reaction (arrow). X 400.

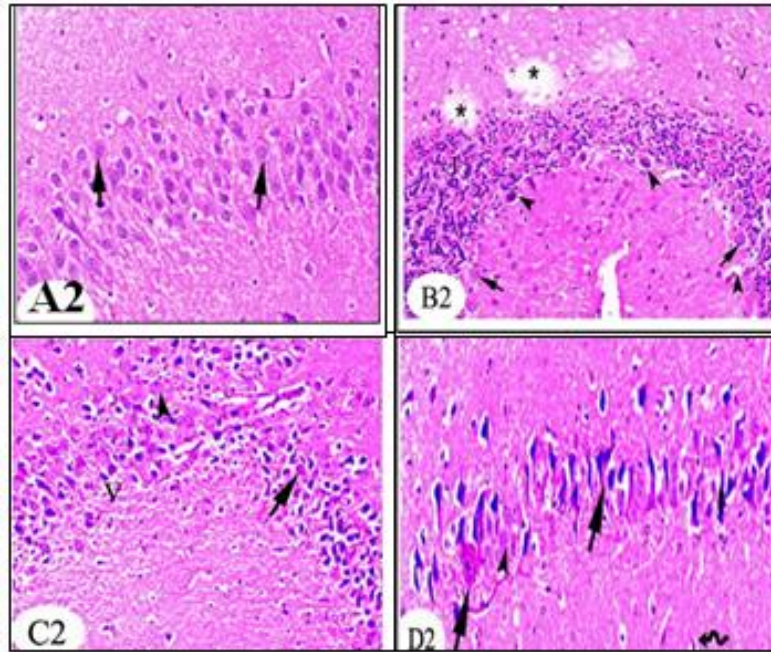


Fig.3. Photomicrographs of the section in the hippocampus of four groups. A2 control hippocampus display densely packed stained Nissl granules in their cytoplasm (arrows) and the different fields of the hippocampal formation. B2. The section in the hippocampus of the subchronic group display necrosis in pyramidal cells in region CA3 (arrowhead) and loss of neurons (*). C2. The section of the chronic hippocampus group displays necrosis in pyramidal cells in region CA3 with vacuolation (V) in pyramidal cells layers. D2. Section of acute hippocampus display necrosis in pyramidal cells in region CA3 with loss of layers of pyramidal cells and odema (*).

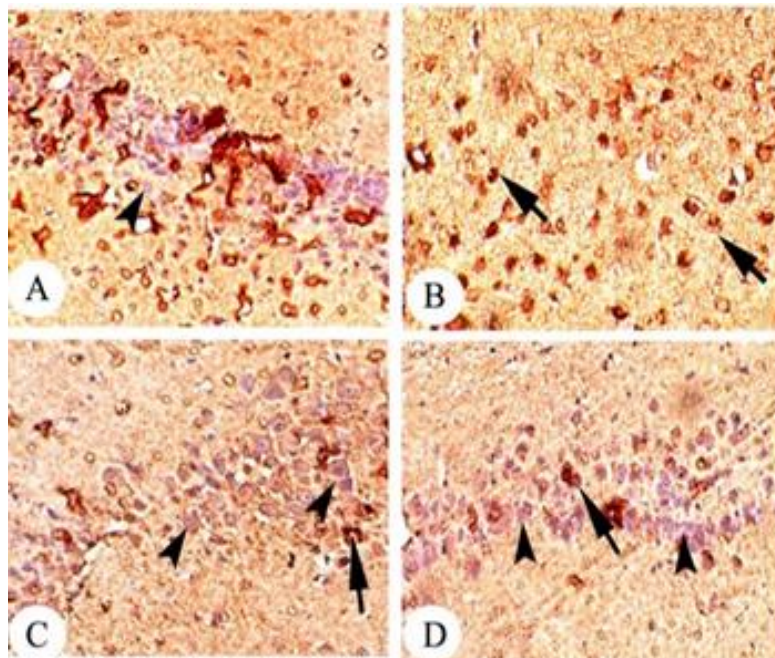


Fig.4. Photomicrographs of p53 immunoreactivity in the hippocampus of different studied groups. A. Control group, B. Subchronic group, C. Chronic group and D. Acute group. The brown color represents a positive p53 reaction in the nuclei of pyramidal cells (arrow) while the blue color represents a nondetectable reaction (arrowhead) X 400.

DISCUSSION

Oganophosphorus pesticides (OPs) are generally used for dealing with pests worldwide, but they lead to oxidative stress which is responsible for several neurological diseases, including Parkinson's disease, seizure, depression, and Alzheimer's disease (Farkhondeh *et al.*, 2020).

In this study we let Wister rats inhale Malathion as a mood of environmental toxicity in different doses subchronic, chronic and acute doses to highlight the relationship between Malathion and oxidative stress which demonstrated an imbalance between free radical production and antioxidant activity increased because of the toxic effect of Malathion and the effect of that in some organs like liver and brain.

Many toxic symptoms were noted obviously during our experiments like irritability, nervousness, diarrhea and frequent urination except control group all groups show these symptoms according to their doses. Many similar symptoms such as sluggishness, muscular tremors, irregular movements, and abdominal tremble were reported by Selmi *et al.* (2015).

The results of the current study showed that Malathion inhalation causes significant decreases in the levels of the SOD, CAT and GPx enzymes, as well as non-enzymatic antioxidants such as TAC and Se in the blood of male Wister rats, compared with the control group reflecting the exhaustion of the cellular antioxidant defense mechanisms.

Previous experimental investigations showed that Malathion induced various biochemical and histological changes in experimental animals (Baiomy *et al.*, 2015; Abdel-Salam *et al.*, 2018; Gupta *et al.*, 2019; Hosseini *et al.*, 2019). OPs can disturb the function of mitochondria by inducing oxidative stress (Farkhondeh, *et al.*, 2020). tried to highlight the role of dysfunction of mitochondria and the induction of oxidative stress in the neurotoxicity induced by Ops, also the inhibitory effects of these pesticides on acetylcholinesterase lead to neurotoxic damages. Moreover, Abdel-Daim *et al.* (2020) showed that Malathion causes a significant decrease in the tissue levels of the nonenzymatic antioxidant (GSH), as well as GPx, SOD, and CAT enzymes in the brain, liver, and kidneys of Malathion intoxicated rats, was observed, which means the depletion of the cellular antioxidant defense.

Comet assay is useful for the detection of DNA strand breaks in mammalian cells (Singh *et al.*, 1988). Single gel cell electrophoresis (Comet assay) is a common method used to measure DNA damage. Comet assay is commonly used as a biomarker for DNA damage; it has been widely used in the field of genetic toxicology and environmental biomonitoring. The DNA damage detected by the comet assay could be due to DNA single-strand breaks, double-strand breaks, adduct formations, DNA-DNA and DNA-protein cross-links (Mitchelmore & Chipman, 1998). However, when DNA damage is beyond the ability of the DNA repair system, the DNA damage is hard to completely repair, and the damage accumulates (Hashimoto *et al.*, 2007).

In this study, the ability of Malathion to cause DNA damage to peripheral blood lymphocytes and liver cells was determined using *the* 'Comet assay'. The indexes of DNA damage (tail length & moment) following subchronic, chronic and acute treatments were increased in a dose-dependent manner in peripheral blood lymphocytes and liver but DNA damage in peripheral blood lymphocytes of the acute group was less than that in chronic. Malathion is a potent toxic pesticide and its exposure can exhibit damage in a dose-dependent manner (Channar *et al.*, 2021).

Our results confirm previous studies indicating increased the DNA damage in peripheral blood lymphocytes after acute and chronic treatment with Malathion where it

was administered intraperitoneally once a day for one day (acute) or for 28 days (chronic) protocols (in both protocols, malathion was administered at 25, 50, 100, and 150 mg/kg) (Reus *et al.*, 2008) and after treatment with organophosphate pesticides (Chlorpyrifos 4 h LC₅₀ 0.2 mg/L, methyl parathion 4 h LC₅₀ 0.135 mg/L, malathion [4 h LC₅₀ > 5.2 mg/L) individually and in a mixture) (Ojha & Srivastava, 2014). *P53* is the gene involved in the regulation of the cell cycle, serving as a checkpoint for the G1-S phase (Duan *et al.*, 2017). However, the p21 gene is existing in the downstream position of the *p53* gene in the signaling pathway and is a CDKI that makes damaged cells stagnate in the G1 phase to reduce the formation of mutations (Takahashi *et al.*, 2014). DNA damage can induce *p53* expression, which can promote the cell cycle arrest by inducing the p21 protein expression, which can directly induce the damaged cells to enter into G1 phase to repair, *p53* and *p21* are the important tumor suppressor genes that play an important role in the development of cancer. If the *p53* or p21 gene changes, they may lead to the functional changes in promoting cell cycle arrest, thus the damaged DNA will not have enough time to repair and the parent cells will pass damaged DNA information to the progeny cells, this causes the genome instability leading to cell malignancy (Ray-Coquard *et al.*, 2012; Huang *et al.*, 2015).

The results here showed decreasing in mRNA expression of both *p53* & *p21* in brain cells which may be explained by the ability of cell damage repair has decreased in the exposed groups. In contrast, in liver cells, mRNA expression levels of the *p53* and *p21* genes were elevated than those in the control group indicating that apoptosis induced by Malathion may depend on the induction and activation of *p53* and *p21* dependency. That is consistent with previous results (Ali *et al.*, 2020) as they notice that *P53* expression levels increased in liver tissue of the male mice when they were treated with the commercial diazinon, the results concluded that not only the organophosphates but also the other byproducts affect the cellular responses to cytokine and apoptotic elements through alteration in the mRNA expression by increasing the levels of free radical generation. Controversially, 180 long-term organophosphorus pesticide exposed workers and 115 healthy controls where the mRNA expression levels of *p53* and *p21* in the exposure group were significantly lower than that in the control group in peripheral lymphocyte DNA (Duan *et al.*, 2017). In previous studies also organophosphorus compounds affected the expression levels of *p53* and p21. In Calaf *et al.* (2021) review recording that the combination of parathion and estrogen down-regulated *p53*, a study analyzed peripheral lymphocyte DNA obtained from 180 workers with long-term exposure to Ops. That study reported that Omethoate, an OP compound, affected the expression of *p53*, which in turn had an impact on the length of the telomere, suggesting a clear influence of pesticides over the cell cycle and tumor formation. Previous experimental investigations showed that Malathion induced various biochemical and histological changes in experimental animals (Baiomy *et al.*, 2015; Abdel-Salam *et al.*, 2018; Gupta *et al.*, 2019; Hosseini *et al.*, 2019).

Our results of real-time PCR of *p53* gene in the brain agree with histopathological and immunohistochemical results of *p53* reaction in hippocampus sections. Examination of normal and treated immunohistochemical examination shows that *p53* expression decrease in hippocampus sections according to their dose mild in subchronic dose, moderate in chronic dose, and high in acute dose. In the hippocampus histopathological sections marked the effect of Malathion appear in the form of cell death markers according to their doses which means that mutation has happened in genes responsible for cell programmed death that could be an alarm for Alzheimer's disease. Focal gliosis and neuronal degenerations in the brain tissues of male Wistar rats were observed in the Malathion group (100 mg kg⁻¹ day⁻¹ by the oral route for 28 days (Akbel

et al., 2018). which was associated with dilatation and conjunction in central vein and portal vein also inflammation in blood sinusoids according to their dose mild in subchronic dose, moderate in chronic and elevated in acute dose. Concurring with the results of real-time PCR of the *p53* gene, hippocampus paraffin sections revealed marked histopathological effects of Malathion in the form of cell death in several areas, with disruption of normal layer organization that could impair memory formation and cognition in the treated rats. The hippocampus is a part of the limbic system. It is responsible for the brain from some drugs but many chemotherapeutic drugs can affect its function by direct or indirect methods 48. memory and learning. The blood-brain barrier protects the immunohistochemical results of *p53* reaction in liver sections showing that *p53* expression increases in liver sections according to their doses, which could be an alarm for liver cancer.

OP also recorded tissues damage in previous studies *et al.* (2010) administered 27 mg kg⁻¹ of Malathion to rats for 28 days, and mononuclear cell infiltration, haemorrhage, calcification, degeneration of the vacuoles, dilation of sinusoids, vascular congestion, and necrosis were observed. In Immunohistochemical detection of cellular tumor antigen *p53* in mammary tissues of albino female rats treated with Malathion twice a day for five days, nuclear *p53* expression in the malignant cells increased by (Omran *et al.*, 2015).

Conclusion

We recommended here forbidding using that kind of old-fashion and harmful pesticide which affect human health, may lead to cancer and replace it with a new generation of Biopesticides and Biotechnology Pesticide Products which use advanced science and are less harmful to human health. It's time for WHO to intervene and outlaw that old fashion harmful pesticide because that is the way to stop producing it.

Conflicts of interest: There are no conflicts to declare.

Acknowledgments: This work was supported by the Faculty of Science, Fayoum University, Fayoum, Egypt

REFERENCES

- Abdel-Daim, M. M., Abushouk, A. I., Bungău, S. G., Bin-Jumah, M., El-Kott, A. F., Shati, A. A., ... & Alkahtani, S. (2020). Protective effects of thymoquinone and diallyl sulphide against malathion-induced toxicity in rats. *Environmental Science and Pollution Research*, 27(10), 10228-10235.
- Abdel-Salam, O. M., Galal, A. F., Hassanane, M. M., Salem, L. M., Nada, S. A., & Morsy, F. A. (2018). Grape seed extracts alone or combined with atropine in treatment of malathion induced neuro-and genotoxicity. *Journal of nanoscience and nanotechnology*, 18(1), 564-575.
- Aebi, H. (1984). Catalase in vitro. *In Methods in enzymology*, (Vol. 105, pp. 121- 126). Academic Press.
- Aggleton, J. P. (2012). Multiple anatomical systems embedded within the primate medial temporal lobe: implications for hippocampal function. *Neuroscience & Biobehavioral Reviews*, 36(7), 1579-1596.
- Akbel, E., Arslan-Acaroz, D., Demirel, H. H., Kucukkurt, I., & Ince, S. (2018). The subchronic exposure to malathion, an organophosphate pesticide, causes lipid peroxidation, oxidative stress, and tissue damage in rats: the protective role of resveratrol. *Toxicology Research*, 7(3), 503-512.
- Ali, N. I., Salem, L. M., Elateek, S. Y., & Khalil, W. K. (2020). Modulation impact of Diazinon forms on gene expression profile and DNA damage pathway in male mice. *Journal of Applied Pharmaceutical Science*, 10(08), 067-074.

- Awadalla, E. A., & Salah-Eldin, A. E. (2016). Molecular and histological changes in cerebral cortex and lung tissues under the effect of tramadol treatment. *Biomedicine & Pharmacotherapy*, 82, 269-280.
- Baiomy, A. A., Attia, H. F., Soliman, M. M., & Makrum, O. (2015). Protective effect of ginger and zinc chloride mixture on the liver and kidney alterations induced by malathion toxicity. *International journal of immunopathology and pharmacology*, 28(1), 122-128.
- Balali-Mood, M., & Saber, H. (2012). Recent advances in the treatment of organophosphorous poisonings. *Iranian journal of medical sciences*, 37(2), 74.
- Banerjee, B. D., Seth, V., Bhattacharya, A., Pasha, S. T., & Chakraborty, A. K. (1999). Biochemical effects of some pesticides on lipid peroxidation and free-radical scavengers. *Toxicology letters*, 107(1-3), 33-47.
- Calaf, G. M., Bleak, T. C., & Roy, D. (2021). Signs of carcinogenicity induced by parathion, malathion, and estrogen in human breast epithelial cells. *Oncology Reports*, 45(4), 1-1.
- Channar, S. P., Qazi, N., Almani, S. A., Memon, S. G., Qazi, M. M., & Qureshi, R. (2021). Histomorphometric Alterations in Hepatic Tissue from Malathion-Induced Toxicity: An Experimental Animal Study. *Journal of Islamabad Medical & Dental College*, 10(1), 370-375.
- Coban, F. K., Ince, S., Kucukkurt, I., Demirel, H. H., & Hazman, O. (2015). Boron attenuates malathion-induced oxidative stress and acetylcholinesterase inhibition in rats. *Drug and chemical Toxicology*, 38(4), 391-399.
- Duan, X., Yang, Y., Wang, S., Feng, X., Wang, T., Wang, P., ... & Wang, W. (2017). Changes in the expression of genes involved in cell cycle regulation and the relative telomere length in the process of canceration induced by omethoate. *Tumor Biology*, 39(7), 1010428317719782.
- Farkhondeh, T., Mehrpour, O., Forouzanfar, F., Roshanravan, B., & Samarghandian, S. (2020). Oxidative stress and mitochondrial dysfunction in organophosphate pesticide-induced neurotoxicity and its amelioration: a review. *Environmental Science and Pollution Research*, 27(20), 24799- 24814.
- Fortunato, J. J., Feier, G., Vitali, A. M., Petronilho, F. C., Dal-Pizzol, F., & Quevedo, J. (2006). Malathion-induced oxidative stress in rat brain regions. *Neurochemical Research*, 31(5), 671-678.
- Gupta, V. K., Siddiqi, N. J., Ojha, A. K., & Sharma, B. (2019). Hepatoprotective effect of Aloe vera against cartap-and malathion-induced toxicity in Wistar rats. *Journal of cellular physiology*, 234(10), 18329-18343.
- Guyton, K. Z., Loomis, D., Grosse, Y., El Ghissassi, F., Benbrahim-Tallaa, L., Guha, N., ... & Straif, K. (2015). International Agency for Research on Cancer Monograph Working Group ILF. Carcinogenicity of tetrachlorvinphos, parathion, malathion, diazinon, and glyphosate. *Lancet Oncol*, 16(5), 490-491.
- Hashimoto, K., Takasaki, W., Sato, I., & Tsuda, S. (2007). DNA damage measured by comet assay and 8-OH-dG formation related to blood chemical analyses in aged rats. *The Journal of toxicological sciences*, 32(3), 249-259.
- Hazarika, A., Sarkar, S. N., Hajare, S., Kataria, M., & Malik, J. K. (2003). Influence of malathion pretreatment on the toxicity of anilofos in male rats: a biochemical interaction study. *Toxicology*, 185(1-2), 1-8.
- heehan, D. C., & Hrapchak, B. B. (1987). Theory and Practice of Histotechnology, Columbus. OH-Battelle Memorial Institute.
- Hosseini, S. A., Saidijam, M., Karimi, J., Azari, R. Y., Hosseini, V., & Ranjbar, A. (2019). Cerium Oxide Nanoparticle Effects on Paraoxonase-1 Activity and

- Oxidative Toxic Stress Induced by Malathion: A Potential Antioxidant Compound, yes, or no? *Indian Journal of Clinical Biochemistry*, 34(3), 336-341.
- Huang, X., Yuan, X., Chen, Z., & Liang, S. (2015). p14ARF enhances cisplatin-induced apoptosis in human osteosarcoma cells in p53-independent pathway. *Zhonghua yi xue za zhi*, 95(35), 2875-2879.
- Ighodaro, O. M., & Akinloye, O. A. (2018). First line defence antioxidants-superoxide dismutase (SOD), catalase (CAT) and glutathione peroxidase (GPX): Their fundamental role in the entire antioxidant defence grid. *Alexandria journal of medicine*, 54(4), 287-293.
- Issam, C., Samir, H., Zohra, H., Monia, Z., & Hassen, B. C. (2009). Toxic responses to deltamethrin (DM) low doses on gonads, sex hormones and lipoperoxidation in male rats following subcutaneous treatments. *The Journal of toxicological sciences*, 34(6), 663-670.
- Kalender, S., Uzun, F. G., Durak, D., Demir, F., & Kalender, Y. (2010). Malathion-induced hepatotoxicity in rats: the effects of vitamins C and E. *Food and Chemical Toxicology*, 48(2), 633-638.
- Koracevic, D.; Koracevic, G.; Djordjevic, V.; Andrejevic, S and Cosic, V. (2001). Method for the measurement of antioxidant activity in human fluids. *Journal of Clinical Pathology*, 54(5):356–361.
- Kumaravel, T. S., & Jha, A. N. (2006). Reliable Comet assay measurements for detecting DNA damage induced by ionizing radiation and chemicals. *Mutation Research/Genetic Toxicology and Environmental Mutagenesis*, 605(1-2), 7-16.
- Mitchelmore CL, Chipman JK (1998) DNA strand breakage in aquatic organisms and the potential value of the comet assay in environmental monitoring. *Mutation Research*, 399:135–147.
- Nishikimi, M.; Roa, N. A and Yogi, K. (1972). Measurement of superoxide dismutase. *Biochemical and Biophysical Research Communication*, 46:849–854.
- Ojha, A., & Srivastava, N. (2014). In vitro studies on organophosphate pesticides induced oxidative DNA damage in rat lymphocytes. *Mutation Research/Genetic Toxicology and Environmental Mutagenesis*, 761, 10-17.
- Olive, P. L., Banáth, J. P., & Durand, R. E. (1990). Detection of etoposide resistance by measuring DNA damage in individual Chinese hamster cells. *JNCI: Journal of the National Cancer Institute*, 82(9), 779-783.
- Omran, O. M., & Omer, O. H. (2015). The effects of alpha-lipoic acid on breast of female albino rats exposed to malathion Histopathological and immunohistochemical study. *Pathology-Research and Practice*, 211(6), 462-469.
- Paglia, D. E and Valentine, W. N. (1967). Studies on the quantitative and qualitative characterization of erythrocyte glutathione peroxidase. *The Journal of Laboratory and Clinical Medicine*. 70:158–169.
- PENNANEN, A., XUe, T., & HARTIKAINEN, H. (2002). Protective role of selenium in plant subjected to severe UV irradiation stress. *Journal of applied botany* (1995), 76(1-2), 66-76.
- Poomagal, S., Sujatha, R., Kumar, P. S., & Vo, D. V. N. (2021). A fuzzy cognitive map approach to predict the hazardous effects of malathion to environment (air, water and soil). *Chemosphere*, 263, 127926.
- Qiu, Y. L., Wang, W., Wang, T., Liu, J., Sun, P., Qian, J., ... & Xia, Z. L. (2008). Genetic polymorphisms, messenger RNA expression of p53, p21, and CCND1, and possible links with chromosomal aberrations in Chinese vinyl chloride–

- exposed workers. *Cancer Epidemiology and Prevention Biomarkers*, 17(10), 2578-2584.
- Ray-Coquard, I., Blay, J. Y., Italiano, A., Le Cesne, A., Penel, N., Zhi, J., ... & Bui, B.N. (2012). Effect of the MDM2 antagonist RG7112 on the P53 pathway in patients with MDM2-amplified, well-differentiated or dedifferentiated liposarcoma: an exploratory proof-of-mechanism study. *The lancet oncology*, 13(11), 1133-1140.
- Reus, G. Z., Valvassori, S. S., Nuernberg, H., Comim, C. M., Stringari, R. B., Padilha, P. T., ... & Quevedo, J. (2008). DNA damage after acute and chronic treatment with malathion in rats. *Journal of agricultural and food chemistry*, 56(16), 7560-7565.
- Saquib, Q., Attia, S. M., Siddiqui, M. A., Aboul-Soud, M. A., Al-Khedhairi, A. A., Giesy, J. P., & Musarrat, J. (2012). Phorate-induced oxidative stress, DNA damage and transcriptional activation of p53 and caspase genes in male Wistar rats. *Toxicology and applied pharmacology*, 259(1), 54-65.
- Selmi, S., Tounsi, H., Safra, I., Abdellaoui, A., Rjeibi, M. R., El-Fazaa, S., & Gharbi, N. (2015). Histopathological, biochemical and molecular changes of reproductive function after malathion exposure of prepubertal male mice. *RSC Advances*, 5(18), 13743-137.
- Shah, M. D., & Iqbal, M. (2010). Diazinon-induced oxidative stress and renal dysfunction in rats. *Food and chemical toxicology*, 48(12), 3345-3353.
- Singh, N. P., McCoy, M. T., Tice, R. R., & Schneider, E. L. (1988). A simple technique for quantitation of low levels of DNA damage in individual cells. *Experimental cell research*, 175(1), 184-191.
- Srikanth, N. S., & Seth, P. K. (1990). Alterations in xenobiotic metabolizing enzymes in brain and liver of rats coexposed to endosulfan and malathion. *Journal of Applied Toxicology*, 10(3), 157-160.
- Takahashi A, Kimura F, Yamanaka A, Takebayashi A, Kita N, Takahashi K and Murakami T: Metformin impairs growth of endometrial cancer cells via cell cycle arrest and concomitant autophagy and apoptosis. *Cancer Cell International*, 14: 53, 2014.
- Tchounwou, P. B., Patlolla, A. K., Yedjou, C. G., & Moore, P. D. (2015). Environmental exposure and health effects associated with malathion toxicity. *Toxicity and Hazard of Agrochemicals*, 51, 2145-9.
- Ukpebor, J., Llabjani, V., Martin, F. L., & Halsall, C. J. (2011). Sublethal genotoxicity and cell alterations by organophosphorus pesticides in MCF-7 cells: Implications for environmentally relevant concentrations. *Environmental Toxicology and Chemistry*, 30(3), 632-639.
- United States. Environmental Protection Agency. Office of Air Quality Planning. (1996). Review of the national ambient air quality standards for particulate matter: Policy assessment of scientific and technical information. DIANE Publishing.
- Verma, R. S., & Srivastava, N. (2001). Chlorpyrifos induced alterations in levels of thiobarbituric acid reactive substances and glutathione in rat brain. *Indian Journal of Experimental Biology*;39(2):174-7.
- Winston, G. W., Regoli, F., Dugas Jr, A. J., Fong, J. H., & Blanchard, K. A. (1998). A rapid gas chromatographic assay for determining oxyradical scavenging capacity of antioxidants and biological fluids. *Free Radical Biology and Medicine*, 24(3), 480-493.